A Correlation between Lamellar Contraction and Applied Shear Stress in Diblock Copolymers

Lei Qiao,† Anthony J. Ryan,‡ and Karen I. Winey*,†

Laboratory for Research on the Structure of Matter, Department of Materials Science and Engineering, University of Pennsylvania, Philadelphia, Pennsylvania, 19104-6272, and Department of Chemistry, University of Sheffield, Sheffield S3 7HF, United Kingdom

Received June 28, 2001; Revised Manuscript Received February 8, 2002

ABSTRACT: We investigate simultaneous lamellar contraction and the stress−strain response in styrene−ethylene propylene (SEP) lamellar diblock copolymer melts under shear. Lamellar contraction was found in predominately parallel lamellae in three SEP copolymers during steady shear. The amount of contraction strongly depends on the molecular weight of the block copolymers as well as the rate of deformation. These molecular weight and shear rate dependences are discussed in terms of chain distortions and entanglements in the interpenetration zones of the block copolymer lamellae. For three molecular weights and three shear rates, we report a unifying correlation between lamellar contraction and applied shear stress, indicating a strong dependence of the molecular-scale chain distortion and the macroscopic strength of deformation (stress).

Introduction

The viscoelastic properties of lamellar block copolymers and polymer brushes under finite shear have been the subjects of many theoretical calculations and simulations in the past few years.[1−6] In particular, Williams and MacKintosh[3] examined the elastic nature of lamellar diblock copolymer chains under shear. They proposed that, in the strong segregation limit as well as at a fast enough shear rate, block copolymer chains distort elastically, giving rise to a reduction in lamellar spacing. Joanny,[2] on the other hand, studied the viscous contribution of the interpenetration zone between two opposing polymer brushes and argued that the viscous friction concentrated in this small interpenetration zone dissipates most of the energy during shear deformation. The first theoretical examination of the interpenetration zone within block copolymer lamellae was made by Witten, Leibler, and Pincus,[1] who estimated the extent of interpenetration (and entanglement) across a lamella as well as the slow stress relaxation process due to the entanglement. Later, the rheology of polymer brushes and lamellar diblock copolymers in either a strongly entangled[2,6] or unentangled[4] state was modeled. More recently, the rheology and nonlinear stress response of multiblock copolymers were modeled by assuming time-dependent conversion of bridge (elastic) to loop (viscous) conformations.[7]

Experimental studies have as well been conducted in attempts to contribute to the understanding of the linear and nonlinear deformation behaviors in block copolymers (see Honeker and Thomas for a recent review[8]), including lamellar block copolymers.[9−11] The large strain deformation drives both the morphology and chain dimensions away from their equilibrium states,[8] which is reflected by domain distortion, enhanced orientation (for unoriented lamellae), and layer contraction.[10,12,13] In particular, Polis and co-workers observed lamellar contraction in oriented lamellar diblock copolymers under steady shear via in situ SAXS.[10] By assuming a linear viscoelastic behavior, they interpreted the observed contraction in terms of local strain profiles within the lamellar microdomains.

In this study, we examine the lamellar contraction under steady shear in three styrene−ethylene propylene lamellar diblock copolymers using an in situ SAXS−rheology method. We find that the lamellar contraction increases with both the molecular weight and shear rate. This result will be interpreted on the basis of the presence of entanglements in the interpenetration zones within diblock copolymer lamellae and the molecular weight and shear rate dependences of the friction force within these interpenetration zones. A direct correlation between the relative lamellar contraction and the macroscopic shear stress is compared to the Williams and MacKintosh theory to support our interpretation.

Experimental Section

Materials. Three lamellar poly(styrene-*b*-ethylene propylene) diblock copolymers were examined in this study, SEP(39-24), SEP(38-62), and SEP(111-83), each number corresponding to the nominal molecular weights (kg/mol) of the PS and PEP blocks, respectively. They were synthesized by selective hydrogenation of PS−PI diblock copolymers by Dr. Steven D. Smith at Proctor & Gamble. All three copolymers have a polydispersity of less than 1.04. Approximately 1 mm thick films of the three copolymers were cast at room temperature from 5 wt % toluene solutions. The films were then dried under vacuum for 24 h at room temperature, followed by 24 h at 120 °C, and annealed at 150 °C for 48 h. Samples were prepared by compression molding at 150 °C for subsequent oscillatory shear and steady shear experiments.

SAXS−Rheology. Simultaneous SAXS−steady shear experiments were performed on beam line 16.1 of the Synchrotron Radiation Source (SRS) at the Daresbury Laboratory, Warrington, U.K. A Rheometrics Solids analyzer (RSAII) with shear sandwich geometry was put into the beamline to measure the stress−strain response during steady shear deformation. To allow for in situ scattering along the neutral direction, special shear-sandwich fixtures were constructed so that the sample is rotated 90° relative to the standard RSAII configuration. The sample dimensions were 12 × 1 × 4 mm^3

† University of Pennsylvania.
‡ University of Sheffield.
* To whom correspondence should be addressed.

10.1021/ma011109+ CCC: $22.00
Published on Web 03/26/2002

along the (1) velocity, (2) velocity-gradient, and (3) neutral directions. A RAPID area detector with 1 μs time resolution was located 3 m from the sample to monitor scattering in the 1*−2* plane.

Large-amplitude oscillatory shear (LAOS) was used to prealign SEP(38-62) and SEP(39-24) into a predominately parallel orientation as follows: (a) SEP(38-62): 1 rad/s, 180 °C, $\gamma = 20\%$ for 20 min, then $\gamma = 40\%$ for 50 min; (b) SEP-(39-24): 1 rad/s, 180 °C, $\gamma = 40\%$ for 30 min. SEP(111-83) was highly oriented after compression molding; therefore, no prealignment procedure was applied. After annealing the samples for 40−50 min, 30 1-s SAXS patterns were collected sequentially that define the reference state for each specimen. Steady shear experiments were then conducted on each specimen at three shear rates (0.001, 0.01, and 0.1 s^{-1}) to a total strain of 60% in the forward direction. SAXS patterns with either 0.5 s (for 0.1 s^{-1}) or 1 s (0.01 and 0.001 s^{-1}) collection times and 10 μs (for 0.01 and 0.1 s^{-1}) or 5 s (for 0.001 s^{-1}) intervals between collections were recorded in situ during each steady shear experiment. Therefore, the strain resolutions between two consecutive SAXS patterns for the three shear rates are 0.6% (for 0.001 s^{-1}), 1% (for 0.01 s^{-1}), and 5% (for 0.1 s^{-1}). Quiescent anneal was conducted in between each constant shear rate experiment to allow sufficient recovery of lamellar spacings. New reference states were collected after these quiescent anneal and just before the next shear deformation.

Results

The SAXS patterns of the starting states of all three materials show highly anisotropic scattered intensity distribution, with maximum intensities centered at zero azimuthal angle ($\mu = 0$) (parallel to the film normal) that indicate predominately parallel orientations in these materials. This predominately parallel orientation was maintained during subsequent shearing experiments, with no substantial changes in the intensity distribution along the arcs following each steady shear/anneal cycle.

Figure 1 shows three plots of integrated scattered intensity as a function of scattering vector q for SEP-(111-83), SEP(38-62), and SEP(39-24) before steady shear. The integration was taken along the q vector over azimuthal angles of $\mu = -10°$ to $\mu = 10°$, using a data analysis program from Daresbury Laboratory. Multiple orders of reflections are clearly observed in these quiescent patterns and the subsequent patterns collected during steady shear deformation. The positional ratios of these reflections all correspond to a lamellar morphology, as expected. For example, SEP(39-24) exhibits six orders of reflections, with positional ratios of 1:2:3:4:5:6:7 that clearly corresponds to a lamellar structure. SEP(38-62) and SEP(111-83) also exhibit a lamellar structure. However, the third- and sixth-order reflections in SEP(38-62) and the second- and fourth-order reflections in SEP(111-83) are weak, due to minima in the form factors for 38% and 52% styrene composition in SEP(38-62) and SEP(111-83), respectively.

We calculated the lamellar spacing both before steady shear and at different strain amplitudes during steady shear. Two (for 0.1 s^{-1}) or five (for 0.01 and 0.001 s^{-1}) consecutive SAXS patterns were added to obtain sufficient intensity to resolve higher order reflections. This resulted in strain resolutions of 3%, 5%, and 10% between consecutive combined SAXS patterns for the shear rates of 0.001, 0.01, and 0.1 s^{-1}, respectively. After background subtraction and Gaussian fitting to the multiple orders of reflections in each combined SAXS pattern, a linear regression method was used to determine the lamellar spacing (D). These lamellar spacings

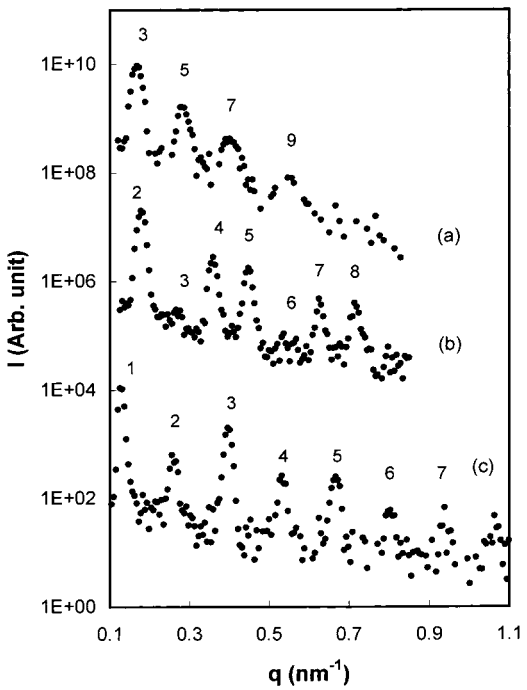

Figure 1. SAXS intensity, I, as a function of scattering vector, q, for (a) SEP(111-83), (b) SEP(38-62), and (c) SEP(39-24), prior to steady shear at 180 °C. The numbers above the peaks represent the nth order reflections. The positional ratios of these reflections all correspond to a lamellar morphology. The first-order reflections in both SEP(111-83) and SEP(38-62) are blocked by the beam stop. The even-order reflections in SEP-(111-83) and the third- and sixth-order reflections in SEP(38-62) coincide with minima in the form factors for 52% and 38% styrene composition, respectively.

at different strain amplitudes were then normalized by the lamellar spacing at zero strain (referred to as the reference state) for each shear rate to give the relative layer spacing, D/D_0, as a function of strain amplitude. As the relative layer spacing decreases, the relative lamellar contraction, $1 - D/D_0$, increases.

Figure 2 shows the relative lamellar spacing (D/D_0) as a function of the macroscopic strain (γ) for the three copolymers. The reference lamellar periods, D_0, for SEP-(39-24), SEP(38-62), and SEP(111-83) are ~45, 70, and 112 nm, respectively, and correspond to the lamellar spacings at zero strain (before steady shear experiment) for each shear rate. The relative lamellar spacing decreases (or the lamellar contraction increases) with increasing macroscopic strain in all three materials at all shear rates, though to different degrees.

Plotted with the same range of D/D_0 (from 0.9 to 1), the measured lamellar spacing shows a strong dependence on the block copolymer molecular weight; that is, the relative lamellar contraction increases with increasing molecular weight of the copolymer. For example, at $\gamma = 60\%$ and 0.1 s^{-1}, the relative lamellar contraction in the lowest molecular weight SEP(39-24) is <1% (Figure 2c), whereas in the highest molecular weight SEP(111-83), an ~8% contraction is observed (Figure 2a). Lamellar contraction increases with increasing shear rate as well, from 1% at 0.001 s^{-1} to ~8% at 0.1 s^{-1} for SEP(111-83).

The simultaneous stress−strain response of the three block copolymers during each steady shear experiment is shown in Figure 3; note the different stress scales along the y-axis. Nonlinear deformation behaviors are observed at large strains. The stress first shows a sharp and almost linear increase with strain, corresponding

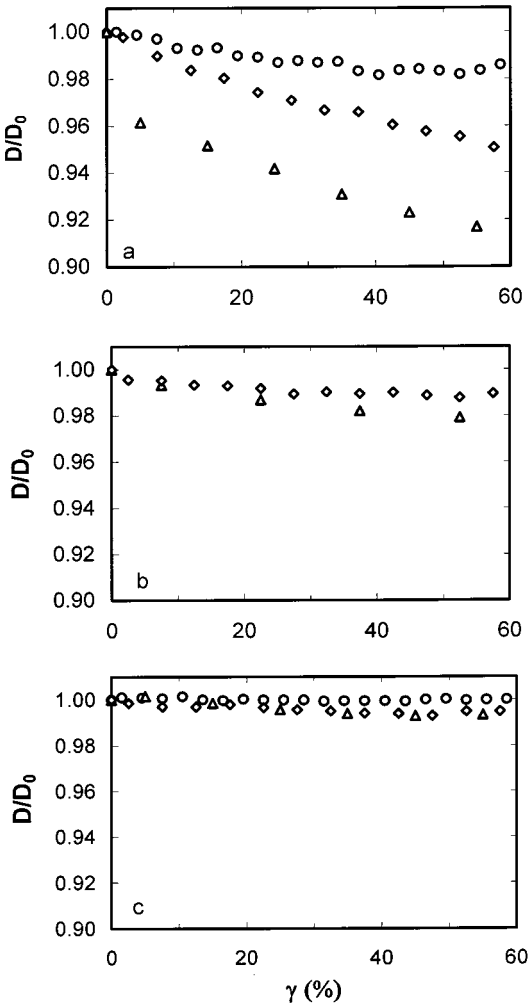

Figure 2. Relative lamellar spacing, D/D_0, as a function of shear strain, γ (%), during steady shear at 180 °C: (a) SEP(111-83), (b) SEP(38-62), and (c) SEP(39-24). Data at three shear rates are shown as (○) for 0.001 s^{-1}, (◇) for 0.01 s^{-1}, and (△) for 0.1 s^{-1}.

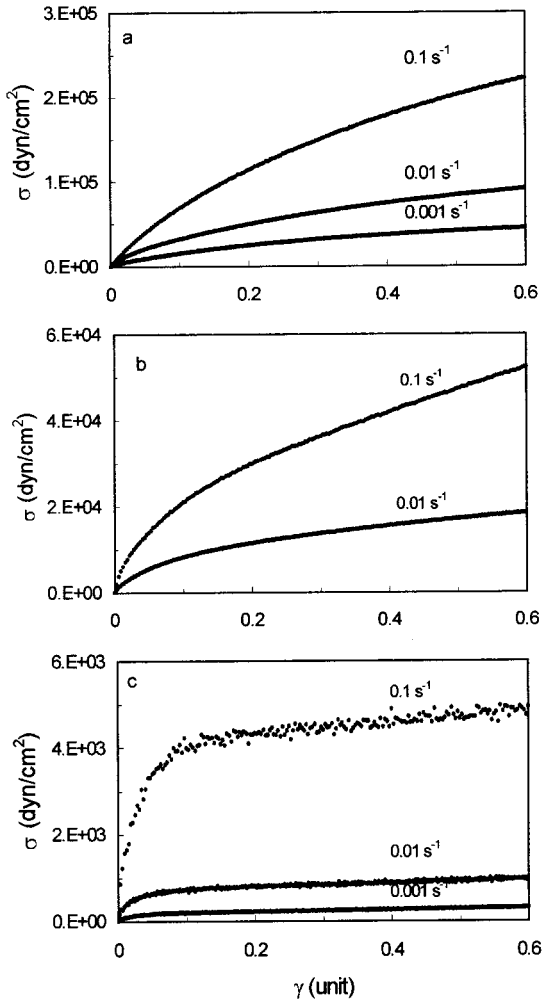

Figure 3. Stress−strain response of three copolymers, (a) SEP(111-83), (b) SEP(38-62), and (c) SEP(39-24), measured during steady shear at 180 °C at three shear rates, 0.001, 0.01, and 0.1 s^{-1}. Note that the stress scales vary considerably between the three plots.

to the linear viscoelastic deformation regime, followed by transition to a slower increase with strain, especially evident for SEP(39-24), indicating the onset of plastic deformation. The shear stress increases with shear strain in all three materials and grows more rapidly in higher molecular weight copolymers. For example, the maximum shear stress (γ = 60% and 0.1 s^{-1}) for SEP(111-83) is nearly 2 orders of magnitude larger than that of the lowest molecular weight SEP(39-24) at the same shearing conditions. Similarly, the shear stress increases with shear rate as well. The maximum shear stress in SEP(39-24) at the highest shear rate, 0.1 s^{-1}, is more than an order of magnitude higher than that at the lowest shear rate, 0.001 s^{-1}.

Before moving on to the discussion, we briefly examine lamellar contraction in a fixed gap experiment. For perfectly parallel lamellae to contract in a fixed gap condition, chains would have to be exchanged between lamellae, which is rather unlikely at the shear rates of our experiments.[14] Alternatively, Williams and MacKintosh predict the loss of the parallel orientation above some critical stress through undulation of lamellae along the direction perpendicular to both the shear and shear gradient direction (i.e., along the neutral dirction) to realize layer contraction in a fixed gap condition.[3] Our experiments cannot evaluate this and similar predictions, because our SAXS geometry only allowed us to monitor orientation distribution parallel to shear and shear gradient direction. Furthermore, as described above and previously, the starting states in our shearing experiments do not possess perfect parallel alignment. The presence of defects, particularly line defects, in our predominately parallel starting state is well documented and contributes to the distribution of orientation.[11,15] (Some of these defects might evolve with shear into kink band defects although it is not the case in this study.[11,15−17]) Preexisting defects could also facilitate the adaptation of lamellae to layer contraction due to elastic chain distortions in a fixed gap experiment.

Discussion

Lamellae contract as a function of shear strain during steady shear and the amount of this contraction strongly depends on both the block copolymer molecular weight and the rate of deformation. The larger the molecular weight and/or the shear rate, the greater the lamellar contraction in the parallel lamellae. We now discuss lamellar contraction in terms of the elastic chain distortion within lamellae.

A theoretical study conducted by Williams and MacKintosh addressed the effects of shear deformation on the lamellar spacing in diblock copolymer melts.[3] Focusing on diblock copolymers in the strong segregation limit, and a deformation rate much faster compared to the rate of chain diffusion (exchange chains between layers), they predicted lamellar contraction under shear as a result of minimizing the equilibrium free energy, including the interfacial free energy and stretching energy.[3] According to their theory, shear induces elastic distortions of the polymer chains, namely chain tilting and stretching, which tend to increase the stretching energy of the system. To reduce the stretching-induced increase in the free energy, the lamellar spacing should decrease. The extent of distortion is measured by the inclination angle of the chains, that is, the strain.[2,4] The larger the shear strain, the more tilting and stretching of the chains and the more contraction in the layer spacing. The observed strain dependence of the relative contraction in our study (Figure 2) is consistent with their prediction; that is, lamellar contraction increases with the applied macroscopic strain.

In addition, we found that lamellar contraction during shear strain also increases with the molecular weight of the block copolymers and the rate of shear. One of the important assumptions in Williams and MacKintosh's theory is uniform stress and strain perpendicular to the parallel lamellae. This is the assumption of linear elastic behavior. As they noted, at larger stresses where interlayer sliding might occur, nonlinear and/or viscoelastic deformation might lead to nonuniform strain profiles across the lamellae. We will now consider the correlation between the interpenetration zone and the shear rate and molecular weight dependence of lamellar contraction.

Previous studies have shown that the rheological behaviors of diblock copolymers under shear are closely related to the presence of a narrow interpenetration zone between like-polymer brushes within microdomains.[1,4] The interpenetration zone helps transmit stress across the lamellae as well as dissipate the shear strain through sliding chains against the opposite chains. After applying a step strain, chains tilt through some inclination angle relative to their original orientation.[4] To relax this distortion, chains from opposite brushes move in the opposite direction, creating a significant frictional force in the interpenetration zone that is the source of the shear stress. As the shear rate increases, viscous strain dissipation in the interpenetration zone decreases, creating a larger degree of chain distortion. Meanwhile, the friction force on chains moving against the opposing brushes as a result of a faster step strain increases. This description of the interpenetration zone implies that both the shear stress and chain distortion (thus lamellar contraction) increases as the strain rate increases, as we observed.

The stretching of chains due to higher shear rates also leads to conformation fluctuations and chains tend to reduce these fluctuations through decreasing the extent of interpenetration or entanglement.[2,4,6] It eventually will reduce the size of the interpenetration zones at large shear rates, leading to a decrease in the sliding viscosity. At sufficiently high shear rates where disentanglement occurs, two different scenarios have been suggested. Joanny[2] predicted a discontinuous jump of viscosity at some critical shear rate where disentanglement occurs, whereas Semenov[4] suggested a smooth power-law decrease of the shear viscosity throughout the nonlinear regime, a gradual shear-thinning process.

Table 1. Molecular Weight (M_{int}) and the Number of Entanglements (M_{int}/M_e) within the Interpenetration Zones of PS and PEP Microdomains, Where M_e Is the Molecular Weight between Entanglements for Homopolymers as Follows: $M_{e,PS} \sim 17.3$ kg/mol and $M_{e,PEP} \sim 1.7$ kg/mol

	M_{int} (kg/mol)		M_{int}/M_e	
	PS block	PEP block	PS block	PEP block
SEP(39-24)	14.2	8.4	<1	~4
SEP(38-62)	14.6	16.5	<1	~9
SEP(111-83)	33.8	22.8	~2	~13

Because we investigated a limited range of shear rates, we cannot distinguish which disentanglement process occurs in our materials.

The molecular weight dependence of lamellar contraction can be explained similarly in terms of chain distortion and its dependence on the interpenetration zone. Previous studies considered the viscous nature of lamellar block copolymers and have shown that entanglement in the interpenetration zone significantly increases the stress relaxation time as well as overall viscosity of lamellar block copolymers.[1,2] Following the approach of Witten, Leibler, and Pincus,[1] we estimate the molecular weights within the interpenetration zones (M_{int}) of the PS and PEP microdomains for the three copolymers (Table 1). For comparison, we compare these molecular weights with the entanglement molecular weights, M_e, for the PS and PEP homopolymers (17 300 and 1660 g/mol, respectively),[15] although M_e is expected to be larger in block copolymer melts due to chain stretching. The number of entanglements within each interpenetration zone is simply M_{int}/M_e. As shown in Table 1, with increasing molecular weight, the interpenetration zones within the PS microdomains change from unentangled in SEP(39-24) and SEP(38-62) ($M_{int}/M_e < 1$) to slightly entangled in SEP(111-83) ($M_{int}/M_e \sim 2$), whereas the interpenetration zones within the PEP domains are more entangled with the number of entanglements increasing with increasing molecular weight. An increase in the molecular weight leads to a higher friction force in the entangled interpenetration zones under shear, therefore leading to an increase in the overall shear stress as well as the degree of chain distortion. This calculation of the extent of entanglement further explains the correlation between the observed stress response and lamellar contraction in these diblock copolymer lamellae.

Semonov considered the elastic nature of block copolymer chains and reached similar conclusions. He suggested two main sources of chain elasticity:[4] one is elasticity due to deformation of the entanglement network (if block copolymer chains are entangled), and the other is due to additional stretching of the chains from conformation fluctuations. In cases where entanglements are not important, that is, the number of links/chains in the interpenetration zone is much less than the number of links between entanglements ($M_{int} \ll M_e$), elasticity is mainly due to the linear stretching of chains normal to the lamellae surface. As the molecular weight of the block copolymer increases to become well entangled within the interpenetration zone, deformation of the entangled network contributes significantly to the elasticity, as in the case of our higher molecular weight SEP block copolymers. In this case, the chain elasticity (or elastic modulus) increases as a result of increasing molecular weight, due to the deformation of increasingly entangled network.[4] This also leads to higher shear stress, as shown in Figure 3, and therefore more chain distortion and lamellar contraction.

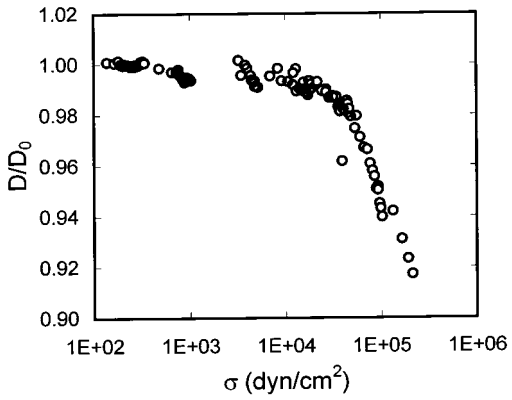

Figure 4. Relative lamellar spacing, D/D_0, as a function of macroscopic shear stress, σ, during steady shear at 180 °C for three copolymers, SEP(111-83), SEP(38-62), SEP(39-24), at three shear rates, 0.1, 0.01, and 0.001 s^{-1}, represented by the same symbol (○), showing that all the data follow the same trend.

It is convenient to employ the definition of the Deborah number, *De*, to qualitatively describe our lamellar contraction results. The Deborah number is often used in dynamic mechanical analysis to compare and predict viscoelastic behaviors in polymers.[18] The definition of *De* is as follows:

$$De = \lambda/t$$

where λ is the time scale of the material's response (or the relaxation time) while t is the time scale of the applied deformation, such as the inverse of the test frequency. The larger *De*, the more elastic the polymer chains behave whereas decreasing *De* makes the material more viscous. For block copolymers under shear, we propose the following approximation for *De*:

$$De \sim \gamma'/\omega_x$$

in which γ' is the macroscopic shear rate and ω_x is the crossover frequency below which chain relaxation occurs. The crossover frequency ($G'(\omega_x) = G''(\omega_x)$) decreases with increasing molecular weight, from ~0.2 rad/s for SEP(39-24) to ≪0.001 rad/s for SEP(111-83). It is evident that increasing either the shear rate γ' or the molecular weight will increase *De*. Thus, as the shear rate or molecular weight increases, the elastic distortion of the chains in response to shear increases, which leads to larger lamellar contraction. The *De* captures qualitatively our result that lamellar contraction increases with strain rate and/or block copolymer molecular weight.

The shear rate and molecular weight dependence of lamellar contraction as well as the simultaneous stress−strain response indicate strong correlation between lamellar contraction and macroscopic shear stress and strain. The stronger the deformation, measured through either an increase in shear stress or strain, the higher the degree of molecular tilting and stretching and therefore the larger the layer contraction. We plot the relative lamellar contraction as a function of the applied shear stress (Figure 4) by using the data in Figures 2 and 3 that provide D/D_0 and shear stress as a function of shear strain. The data from three molecular weights and three shear rates follow a common trend. This direct correlation between the shear stress and lamellar contraction is in qualitative agreement with Williams and MacKintosh's prediction (eq 10 in ref 3). Quantitative agreement between their eq 10 and our data is not achieved due to the complex shear rate and molecular weight dependence of the modulus in these materials. However, the conclusion that the observed lamellar contraction depends more strongly on the macroscopic shear stress than shear strain is unifying. The macroscopic shear stress determines the strength of deformation, and therefore the extent of chain distortion, which is manifested through layer contraction. Excessive stress leads to excessive contraction and might even lead to melt fracture due to increasing distortion or undulation of lamellae.

Conclusion

This study has investigated lamellar contraction in SEP diblock copolymers under shear. Lamellar contraction, due to the elastic chain distortion, namely tilting and stretching during shear deformation, has a strong dependence on both the molecular weight of the copolymers and the rate of deformation. The shear rate dependence of contraction is discussed in terms of friction force and its correlation with the interpenetration zone within block copolymer lamellae. The molecular weight effect on lamellar contraction is closely related to the increasing degree of entanglement in the interpenetration zone and therefore a larger friction force as well as more chain distortion. We found a direct correlation between lamellar contraction and the applied shear stress, indicating that the stress (rather than strain) determines the strength of deformation, and thereby the extent of molecular chain distortion, or lamellar contraction.

Acknowledgment. The authors thank Dr. S. D. Smith of Proctor & Gamble for providing the diblock materials and Dr. A. Gleeson and Dr. N. Terrill of the Daresbury Laboratory for helping us with the in situ SAXS experiments. The authors thank D. R. M. Williams for insightful comments on the manuscript. Funding was provided by NSF-MRSEC (00-79909), NSF-International (99-04127), and EPSRC (GR/M22116).

References and Notes

(1) Witten, T. A.; Leibler, L.; Pincus, P. A. *Macromolecules* **1990**, *23*, 824.
(2) Joanny, J. F. *Langmuir* **1992**, *8*, 989.
(3) Williams, D. R. M.; MacKintosh, F. C. *Macromolecules* **1994**, *27*, 7677.
(4) Semenov, A. N. *Langmuir* **1995**, *11*, 3560.
(5) Semenov, A. N.; Subbotin, A. V.; Hadziioannou, G.; Brinke, G. T.; Manias, E.; Doi, M. *Macromol. Symp.* **1997**, *121*, 175.
(6) Rubinstein, M.; Obukhov, S. P. *Macromolecules* **1993**, *26*, 1740.
(7) Ganesan, V.; Fredrickson, G. H. *J. Rheol.* **2001**, *45*, 161.
(8) Honeker, C. C.; Thomas, E. L. *Chem. Mater.* **1996**, *8*, 1702.
(9) Dair, B. J.; Honeker, C. C.; Alward, D. B.; Avgeropoulos, A.; Hadjichristidis, N.; Fetters, L. J.; Capel, M.; Thomas, E. L. *Macromolecules* **1999**, *32*, 8145.
(10) Polis, D. L.; Winey, K. I.; Ryan, A. J.; Smith, S. D. *Phys. Rev. Lett.* **1999**, *83*, 2861.
(11) Qiao, L.; Winey, K. I. *Macromolecules* **2000**, *33*, 851.
(12) Pinheiro, B. S.; Winey, K. I.; Hajduk, D. A.; Gruner, S. M. *Macromolecules* **1996**, *29*, 1482.
(13) Yamaoka, I.; Kimura, M. *Polymer* **1993**, *34*, 4399.
(14) Lodge, T. P.; Dalvi, M. C. *Phys. Rev. Lett.* **1995**, *75*, 657.
(15) Polis, D. L.; Winey, K. I. *Macromolecules* **1998**, *31*, 3617.
(16) Polis, D. L.; Winey, K. I. *Macromolecules* **1996**, *29*, 8180.
(17) Qiao, L.; Winey, K. I.; Morse, D. C. *Macromolecules*, in press.
(18) Menard, K. P. *Dynamic Mechanical Analysis: A Practical Introduction*; CRC Press: Boca Raton, FL, 1999.

MA011109+